

# Modulated photocurrent as a powerful method to reveal predominant transport by the majority carriers of disordered semiconductors and to resolve all the kinds of probed gap states

M. Pomoni, A. Giannopoulou, P. Kounavis \*

*Department of Engineering Sciences, School of Engineering, University of Patras, 26504 Patra, Greece*

Available online 28 January 2008

## Abstract

A basic difficulty in the interpretation of photoconductivity measurements may arise from possible mixed contributions of both carriers to the photocurrent. In this work it is demonstrated that a universal behavior in the simulated spectra of the out of phase modulated photocurrent signal is observed in cases where the majority carriers dominate. In these cases, a general formula can be used to evaluate the densities of various species of states using the data from all frequencies. Deviations from the universal behavior can be observed when there are contributions from both carriers. The applicability of our analysis is demonstrated in a-Si:H.

© 2008 Elsevier B.V. All rights reserved.

*PACS:* 72.20.Jv; 72.80.Ng; 73.61.Jc

*Keywords:* Silicon; Defects; Photoconductivity

## 1. Introduction

Various techniques based on photoconductivity measurements are widely used to investigate the optoelectronic properties of disordered semiconductors. However, there are usually difficulties in the interpretation of the results because of possible mixed contributions to the photocurrent from both carriers. In this work, it is shown that this limitation may be overcome in the modulated photocurrent (MPC) experiment. This is demonstrated by examining the characteristics of simulated out of phase MPC spectra in various cases where one or both carriers dominate. Distinct characteristics are found in these spectra that can be used to reveal whether the interaction of the majority carriers with the probed states dominates. In this case, a general formula can be used for a density of states (DOS) spectroscopy of the various species of probed states. The applicability of our analysis is demonstrated in a-Si:H.

## 2. Results of simulations

In our theoretical analysis of the MPC experiment we have shown [1] that the essential parameter is the out of phase MPC  $Y$  signal which is obtained by means of phase shift ( $\Phi$ ) and modulated photoconductivity ( $\sigma_{ac}$ ) using  $Y = \mu e G_{ac} \sin \Phi / \sigma_{ac}$ , where  $\mu$  is the mobility of the majority carriers and  $G_{ac}$  the modulated light generation rate. If the interaction of the majority carriers, electrons for example, with the gap states dominates the  $Y$  signal, then this signal can be directly related to the total effective trapping rate ( $1/\tau_{on}$ ) of the electrons into all the probed gap state distributions  $D^i(E_{\omega}^i)$  above the Fermi level  $E_F$  at the probe rate depths  $E_{\omega}^i$  below the conducting states according to [1]

$$Y = 1/\tau_{on} = (\pi/2) \Sigma_i H(\omega, \omega_i^i) c_n^i D^i(E_{\omega}^i) kT, \quad (1)$$

where  $H(\omega, \omega_i^i) = 1 - (2/\pi) \arctan(\omega_i^i/\omega)$  is the so-called  $H$  function [1], which is a step-like function with a step at  $\omega_i^i$  and determines the effective capture rate into each  $E_{\omega}^i$ .  $E_{\omega}^i$  is given by  $E_{\omega}^i = kT \ln[c_n^i N_C / (\omega^2 + (\omega_i^i)^2)^{1/2}]$ , where  $kT$  is the thermal energy and  $N_C$  is the density of states at the

\* Corresponding author. Tel.: +30 2610996281; fax: +30 2610966260.  
E-mail address: [pkounavis@des.upatras.gr](mailto:pkounavis@des.upatras.gr) (P. Kounavis).

conduction band edge  $E_C$ .  $\omega_i^j$  is the characteristic frequency defined by  $\omega_i^j = nc_n^i + pc_p^i$ , where  $n(p)$  is the density of the free electrons (holes) and  $c_n^i(c_p^i)$  is the capture coefficient for electrons (holes). Since electrons are the majority carriers we assume  $\omega_i^j = nc_n^i$ . The effective capture rate  $1/\tau_{\omega p}$  of holes into the  $D^i(E_\omega)$  below  $E_F$  is also given by the right hand side of Eq. (1) if  $c_n^i$  is replaced by  $c_p^i$ . If the  $Y$  signal is governed by Eq. (1), then a DOS spectroscopy is possible using

$$D^i(E_\omega^i) = (2/\pi)(Y/\mu)\sigma_p/[e\omega_i^j H(\omega, \omega_i^j)kT], \quad (2)$$

where  $\sigma_p$  is the dc photoconductivity. As it is shown here the above formula has the advantage that it can provide the various species of  $D^i(E_\omega^i)$  distributions using the MPC data from all the frequencies. In this work, we examine when the  $Y$  signal is governed by Eq. (1) so that Eq. (2) can be applied. For this purpose, the spectra of  $Y$  signal are generated at 300 K from the exact expressions of the MPC as demonstrated in Ref. [1]. Various models of DOS are introduced to understand mainly the essential behavior of the  $Y$  signal when one or both carriers dominate rather than to fit experimental spectra. The so-generated  $Y$  spectra are compared with those calculated from Eq. (1).

Fig. 1 presents the basic  $D^v(E)$  (closed circles) and  $D^c(E)$  (open circles) distributions below and above  $E_F$ , respectively, introduced in our simulations. The superscripts  $v$  and  $c$  denote the valence and conduction band side of the energy gap. The above states include exponential valence and conduction band tails with characteristic energies of 35 meV and Gaussian distributions, having a width of 0.3 eV and a maximum at 0.7 and 1.3 eV at the density of  $10^{17} \text{ cm}^{-3} \text{ eV}^{-1}$ . The effect of additional species of states is examined by incorporating the Gaussian distributions  $D^{lv}(E)$  and  $D^{hc}(E)$  (broken lines) having a width of 0.3 and 0.1 eV, respectively. These distributions present a maximum at 0.7 and 1.2 eV at the density  $7 \times 10^{16}$  and  $1 \times 10^{16} \text{ cm}^{-3} \text{ eV}^{-1}$ , respectively. The letters  $h$  and  $l$  in the superscripts denote the high and low capture coefficients of these states. All the capture coefficients of the various DOS models are summarized in Table 1.

The DOS model I includes only the  $D^v(E)$  and  $D^c(E)$  distributions of Fig. 1 (circles) with equal densities. This model gives comparable effective capture times  $\tau_{\omega n}$  and  $\tau_{\omega p}$  of electrons and holes, respectively. The  $E_F$  level (arrow) is slightly above the midgap (vertical line), so that the electrons are the majority carriers. If the mobility of electrons ( $\mu_n$ ) and holes ( $\mu_p$ ) are equal, then the mobility

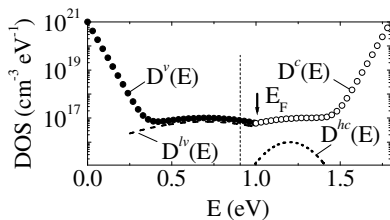


Fig. 1. Gap state distributions used in the DOS model I (circles), model II (circles and dotted line) and model III (circles and dashed line).

Table 1  
Capture coefficients in units of  $\text{cm}^3/\text{s}$  used in the DOS models

	Model I	Model II	Model III
$c_n^v$	$1-20 \times 10^{-8}$	$1-20 \times 10^{-9}$	$1 \times 10^{-8}$
$c_p^v$	$1 \times 10^{-7}$	$1 \times 10^{-7}$	$1 \times 10^{-7}$
$c_n^c$	$1 \times 10^{-7}$	$1 \times 10^{-8}$	$1 \times 10^{-7}$
$c_p^c$	$1 \times 10^{-8}$	$1 \times 10^{-9}$	$1 \times 10^{-8}$
$c_n^{hc}$	–	$1 \times 10^{-6}$	–
$c_p^{hc}$	–	$1 \times 10^{-7}$	–
$c_n^{lv}$	–	–	$1 \times 10^{-10}$
$c_p^{lv}$	–	–	$1 \times 10^{-8}$

effective capture time products of electrons and holes are comparable,  $\mu_n \tau_{\omega n} \approx \mu_p \tau_{\omega p}$ . In this case, as is shown in Fig. 2(a)  $Y$  is not given by Eq. (1) as it differs from the effective capture rates of electrons  $1/\tau_{\omega n}$  and holes  $1/\tau_{\omega p}$ , due to mixed contributions from both carriers. A similar behavior is observed in Fig. 2(a) when the minority carriers dominate. This is accomplished by assuming that  $\mu_p = 10\mu_n$  and so  $\mu_n \tau_{\omega n} \ll \mu_p \tau_{\omega p}$ . The above cases can be recognized from the behavior of the normalized ratio  $Y/Y_0$  in Fig. 2(c). This ratio is obtained if each value of  $Y$  spectrum of a given trap depth  $E_\omega$  is divided by the respective value from the  $Y_0$  spectrum of the same trap depth. The  $E_\omega^c$  is obtained from the above-mentioned expression of  $E_\omega^i$  if  $\omega_i^j$  is replaced by the frequency  $\omega_i^H$ , which is determined as described below. The  $Y_0$  is obtained using the density  $n = 10^8 \text{ cm}^{-3}$  near dark equilibrium such that most frequencies become  $\omega \gg \omega_{i0}^c$  and  $H(\omega, \omega_{i0}^c) = 1$ . Hence from the  $Y$  spectra calculated from Eq. (1), which in our example is dominated by the  $D^c(E)$ , we get  $Y/Y_0 = H(\omega, \omega_i^c)$ . In Fig. 2(c) the ratio  $Y/Y_0$  (dashed lines), extracted from the spectra of Fig. 2(a), as a function of the normalized frequency  $\omega/\omega_i^H$  differs from the universal spectrum of  $H$  function for  $\omega > \omega_i^H$ , indicating that the  $Y$  signal cannot be described by Eq. (1). On the other hand, if it is assumed  $\mu_n = 10\mu_p$ , such that  $\mu_n \tau_{\omega n} \gg \mu_p \tau_{\omega p}$ , then the majority

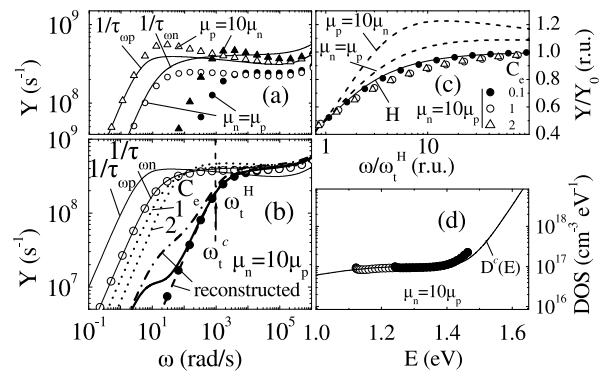


Fig. 2. Calculated spectra of  $Y$  from the DOS model I for  $C_e = 0.1$  and  $n = 10^8 \text{ cm}^{-3}$  (open symbols) and  $10^{10} \text{ cm}^{-3}$  (closed symbols),  $1/\tau_{\omega n}$  and  $1/\tau_{\omega p}$  rates (solid lines), for  $n = 10^8 \text{ cm}^{-3}$  using  $\mu_n \leq \mu_p$  and  $\mu_n = 10\mu_p$  in (a) and (b), respectively. Normalized spectra of  $Y/Y_0$  (symbols) deduced from the  $Y$  spectra presented in (a) and (b) and the spectrum of  $H$  function (solid line) in (c). Evaluated DOS (circles) from the respective  $Y$  spectra (circles) of (b) and introduced DOS (solid line) in the energy domain in (d).

carriers dominate, providing that the capture coefficient ( $c_n^v$ ) for the majority carriers of the states below  $E_F$  are much lower than that ( $c_n^c$ ) of the states above  $E_F$ . This is demonstrated with the  $Y$  signal (symbols) of Fig. 2(b) evaluated for  $C_e = c_n^v/c_n^c = 0.1$  which agrees with the effective capture rate of electrons  $1/\tau_{on}$ . This case can be recognized from the agreement of  $Y/Y_0$  spectrum (solid circles) in Fig. 2(c) with the universal spectrum of  $H$  function, indicating that the  $Y$  signal is given by Eq. (1). According to Eq. (1) around the characteristic frequency  $\omega_t^c$  the  $Y$  signal is dominated by the decay of  $H$  function and this is used to determine  $\omega_t^c$ . Specifically, at the frequency  $\omega_t^H = \omega_t^c$  the  $Y$  signal in Fig. 2(b) has been decreased by a factor of 2 due to the decay of the  $H$  function from the respective value of the  $Y_0$  spectrum with the same trap depth that is at  $1.4 \omega_t^c$  [1]. The so-determined frequency  $\omega_t^H$  can be introduced in the general relation

$$c_n^i = e\omega_t^i\mu/\sigma_p, \quad (3)$$

to determine the capture coefficient  $c_n^c$ . In this case, as it is shown in Fig. 2(d) the probed  $D^c(E)$  is successfully reconstructed (circles) using Eq. (2) by means of all the  $Y$  values from Fig. 2(b) and replacing  $\omega_t^i$  by  $\omega_t^H$ .

On the other hand, if  $C_e = c_n^v/c_n^c > 0.1$ , then the  $Y$  signal is lower than the  $1/\tau_{on}$ . This is demonstrated by the spectra of Fig. 2(b) (dotted lines), generated from the DOS model I by assuming that  $C_e = 1$  and 2 obtained by increasing  $c_n^v$ . These spectra are not appropriate for a DOS spectroscopy. This can be recognized in Fig. 2(c) from the fact that the respective  $Y/Y_0$  ratio (open symbols) is below the  $H$  function for  $\omega > \omega_t^H$ .

Next the effect of various species of probed states is examined using the DOS model II, which apart from the  $D^c(E)$  and  $D^v(E)$  distributions of Fig. 1 includes also the  $D^{hc}(E)$  distribution above  $E_F$  with a relatively low density. This distribution has a capture coefficient  $c_n^{hc}$  for the majority carriers by 2 orders of magnitude higher than the respective  $c_n^c$  of the  $D^c(E)$ , as indicated in Table 1. Thus the capture rate of electrons into the states of  $D^{hc}(E)$  with the lower density dominates over that into the states of  $D^c(E)$ . It is assumed that  $\mu_n = 10\mu_p$  and so  $\mu_n\tau_{on} \gg \mu_p\tau_{op}$ . The capture coefficient  $c_n^v$  for the majority carriers of the gap states below  $E_F$  is taken much lower than the capture coefficients of the states above midgap, namely  $C_e \leq 0.1$ , whereas  $c_p^v > c_n^v$  (see Table 1). In this case, the calculated  $Y$  signal (symbols) of Fig. 3(a) agrees with the effective capture rate  $1/\tau_{on}$  of electrons (majority carriers). In addition, for  $\omega < \omega_t^H$  the  $Y$  spectrum of Fig. 3(a) presents a decay well above that calculated from Eq. (1) (dashed-dotted line) by assuming the single type of states  $D^{hc}(E)$ . This behavior is the signature of the existence of various species of states. The frequency  $\omega_t^H$ , determined according to the method mentioned above, coincides with the characteristic frequency  $\omega_t^{hc}$  of the states with the higher capture coefficient  $c_n^{hc}$ . Thus  $\omega_t^H$  can be introduced in Eq. (3) to determine  $c_n^{hc}$ .

The DOS is evaluated from the formula of Eq. (2) by means of  $Y$  signal of Fig. 3(a) and by replacing  $\omega_t^i$  with

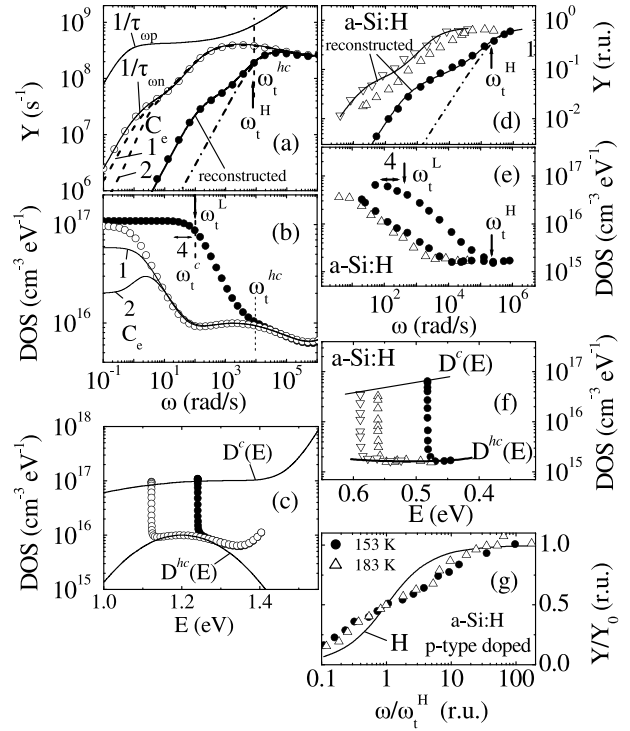


Fig. 3. Calculated spectra of  $Y$  from the DOS model II for  $n = 10^8 \text{ cm}^{-3}$  (open circles) and  $n = 10^{10} \text{ cm}^{-3}$  (solid circles)  $\text{cm}^{-3}$ ,  $1/\tau_{on}$  and  $1/\tau_{op}$  rates (solid lines) for  $n = 10^8 \text{ cm}^{-3}$  in (a). DOS distributions evaluated from the  $Y$  spectra of (a) (circles) in the frequency domain in (b) and energy domain in (c) and introduced DOS (solid lines) in (c). Experimental  $Y$  spectra (d) of a-Si:H from Ref. [2] and calculated DOS in the frequency domain in (e) and energy domain in (f). Comparison of the experimental  $Y/Y_0$  spectra (symbols) of lightly p-type doped a-Si:H of Ref. [3] with the spectrum of  $H$  function in (g).

$\omega_t^H$ . The results are demonstrated in Fig. 3(b) and (c) in the frequency and energy domains, respectively. As it can be seen from Fig. 3(c) the calculated DOS from the data of higher frequencies  $\omega \geq \omega_t^H$  reproduces the  $D^{hc}(E)$  with the higher capture coefficient  $c_n^{hc}$ . Upon decreasing  $\omega$  in the interval  $\omega_t^c < \omega < \omega_t^H$  Eq. (2) gives a growing DOS. This DOS results from the fact that the frequency dependence of  $H$  function dominates in Eq. (2) over the weaker dependence of  $Y$  signal arising from the effective capture rates of electrons into the  $D^c(E)$  and  $D^{hc}(E)$  distributions. Note that such a growing DOS is not observed in the example of Fig. 2(d), because a single type of states is probed. Finally, in the low frequency (LF) regime, which is practically for  $\omega \leq \omega_t^c/4$ , the calculated DOS presents a saturation in Fig. 3(c) and a plateau in Fig. 3(b), which can be used to define the LF regime. Thus the frequency  $\omega_t^L$  which is by a factor of 4 above the onset of the LF regime can be used to determine the characteristic frequency  $\omega_t^c$  and subsequently the  $c_n^c$  from Eq. (3). The saturated value of the calculated DOS in the LF regime gives practically the  $D^c(E)$  with the lower capture coefficient dominating in this regime. The accuracy of the extracted DOS of Figs. 2(d) and 3(c) is verified from the fact that the respective reconstructed  $Y$  spectra (dashed lines) in Figs. 2(b) and 3(a),

evaluated from Eq. (1) and the extracted DOS parameters, agree with the introduced  $Y$  spectra.

Upon increasing  $c_n^v$  in the DOS model II, the  $Y$  signal becomes lower than the effective capture rate of electrons  $1/\tau_{con}$  at low  $\omega$ . This is demonstrated with the examples of Fig. 3(a) (dotted lines) obtained for  $C_e = c_n^v/c_n^c = 1$  and 2. By introducing the so-generated  $Y$  in Eq. (2), the  $D^{hc}(E)$  is reproduced, whereas the  $D^c(E)$  is underestimated, especially for  $C_e = 2$ . This case can be recognized from the calculated DOS in the LF regime of Fig. 3(b) which presents a decay instead of a plateau, because of the stronger decay of  $Y$  than that of  $H$  function.

Finally, it is examined the case of various species of states below  $E_F$  as in the DOS model III. In this model apart from the  $D^c(E)$  and  $D^v(E)$  distributions of Fig. 1 the  $D^{lv}(E)$  distribution below  $E_F$  is incorporated. A similar general behavior was observed with that found in the above examples. Specifically, if  $c_n^v$  and  $c_n^{lv}$  are both lower than  $c_n^c$  and  $\mu_n = 10\mu_p$ , the  $Y$  signal agrees with the  $1/\tau_{con}$ , whereas  $Y$  becomes lower than  $1/\tau_{con}$  when  $c_n^v$  and  $c_n^{lv}$  are equal or higher than  $c_n^c$  (not shown). However, in the extreme case where the  $c_n^{lv}$  of the  $D^{lv}(E)$ , having the lower capture coefficient for the minority carriers ( $c_p^{lv} < c_p^v$ ), is more than 10 times lower than the  $c_n^v$  as indicated in Table 1, the  $Y$  signal presents a clear additional step at low  $\omega$  as is shown in Fig. 2(b) (thick solid line). The spectra present a step-like behavior as that of the spectra of model II and can be attributed erroneously to various species of states above  $E_F$ . However, the additional step is so sharp so that the reconstructed  $Y$  spectrum (dashed-dotted line) evaluated from Eq. (1) using the DOS deduced from Eq. (2) differs from the original  $Y$  spectrum, indicating that the evaluated DOS is not reliable. Similarly, a step-like behavior in the  $Y$  spectra sharper than that calculated by Eq. (1) was also observed in the case of DOS model II assuming that  $c_p^v \leq c_p^v$  (not shown). In general, our simulations showed that if the  $Y$  signal differs from the effective trapping rate of the majority carriers, then the  $Y$  spectra cannot be reconstructed by means of Eq. (1) and the extracted DOS.

### 3. Comparison with experimental spectra

Fig. 3(d) presents typical experimental  $Y$  spectra of undoped a-Si:H presented in Fig. 1 of Ref. [2]. It can be seen a qualitatively very similar behavior with that of the respective simulated spectra presented in Fig. 3(a), indicating that the majority carriers interact with various species of states. Indeed, the DOS evaluated from Eq. (2) presented in the

frequency and energy domains in Fig. 3(e) and (f), respectively, consists of two species of states  $D^c(E)$  and  $D^{hc}(E)$ . These states have very different capture coefficients  $c_n^c = 1.7 \times 10^{-9} \text{ cm}^3/\text{s}$  and  $c_n^{hc} = 1 \times 10^{-6} \text{ cm}^3/\text{s}$ , which are evaluated from the frequencies  $\omega_i^H$  and  $\omega_i^L$  determined from the spectra of Fig. 3(d) and (e) according to the above described methods. Based on the derived DOS parameters the experimental  $Y$  spectra are successfully reconstructed by means of Eq. (1) (solid lines in Fig. 3(d)). This verifies that the majority carriers (electrons) dominate MPC, and  $Y = 1/\tau_{con}$ , so that our DOS spectroscopy is reliable.

Finally, Fig. 3(g) shows the normalized  $Y/Y_0$  spectra of lightly p-type doped a-Si:H extracted from the MPC data of Kleider et al [3]. It can be seen that the  $Y/Y_0$  spectra are very different from the universal spectrum of the  $H$  function. This indicates that the experimental  $Y$  signal cannot be described by Eq. (1), suggesting that there are contributions from both carriers, which are reasonable for this lightly doped material.

### 4. Conclusion

A DOS spectroscopy based on Eq. (2) can be applied to determine the DOS parameters of the various species of states with which the majority carriers interact, as far as the  $Y$  signal agrees with the effective trapping rate of the majority carriers into the probed states. It is deduced that this limitation is fulfilled as far as the experimental  $Y$  signal can be reconstructed by means of Eq. (1) and the extracted DOS parameters. In such a case, the  $Y$  signal is found to follow the universal frequency dependence of the  $H$  function around each characteristic frequency  $\omega_i^j$ . By contrast, if the reconstructed  $Y$  signal differs from the experimental  $Y$  signal, the above limitation is not fulfilled and a DOS cannot be extracted. The applicability of our analysis was demonstrated in the experimental spectra of undoped and lightly p-type doped a-Si:H.

### Acknowledgement

The present work was supported by the ‘K. Karatheodory’ B386/2004 project.

### References

- [1] P. Kounavis, Phys. Rev. B 64 (2001) 45204.
- [2] P. Kounavis, J. Non-Cryst. Solids 352 (2006) 1068.
- [3] J.P. Kleider, C. Longeaud, Solid State Phenom. 44/46 (1995) 596.